

Effect of low-temperature annealing and deformation on the structure of metallic glasses by X-ray diffraction

Y. WASEDA

Department of Metallurgy and Materials Science, University of Toronto, M5S 1A4, Canada

T. EGAMI

Department of Metallurgy and Materials Science and Laboratory for Research on the Structure of Matter, University of Pennsylvania, Philadelphia, Pennsylvania 19104, USA

The changes in the atomic structure of amorphous Pd–Si and Ni–P alloys due to low-temperature annealing, cold-rolling and isothermal creep have been studied by the conventional X-ray diffraction. The present results on the effect of low-temperature annealing were consistent with those of amorphous $\text{Fe}_{40}\text{Ni}_{40}\text{P}_{14}\text{B}_6$ alloy studied by the energy dispersive X-ray diffraction method. In addition, the present results have indicated that the effect of cold-rolling causes small changes in the structure of amorphous $\text{Pd}_{80}\text{Si}_{20}$ alloy which are qualitatively different from the structural relaxation, and the effect of annealing plays a significant contribution in the structural change during an isothermal creep test.

1. Introduction

As a result of studies on metallic glasses in recent years, it became clear that many of their physical properties are often significantly dependent upon the thermal and mechanical history of the sample. In particular, the class of metallic glasses obtained by rapid quenching from the melt show large changes in mechanical and magnetic properties when annealed at temperatures sufficiently low as not to cause crystallization [1]. Many of these changes are believed to be due to structural relaxation, similar to those observed in polymeric glasses [2]. However, since the changes in the atomic structure are rather small and difficult to observe, no reliable structural study of the relaxation process has been in existence until quite recently, when the presence of the structural change was detected [3], and the change was studied in detail to unravel the mechanism of structural relaxation [4, 5] using the energy-dispersive X-ray diffraction technique.

In the present paper, we describe the effect of low-temperature annealing on the structure of

splat-cooled amorphous $\text{Pd}_{80}\text{Si}_{20}$ and $\text{Ni}_{82}\text{P}_{18}$ and electrodeposited amorphous $\text{Ni}_{81}\text{P}_{19}$, to check the accuracy and the generality of the previous studies [4, 5], and furthermore we examine the effects of cold-rolling and isothermal creep on amorphous $\text{Pd}_{80}\text{Si}_{20}$. It has been suggested that annealing and mechanical deformation would have opposite effects on the properties of amorphous alloys [6, 7]. We will examine if this holds true for the structure as well. The studies were carried out with the conventional high-accuracy X-ray diffraction unit [8].

2. Experimental details

The amorphous samples of $\text{Pd}_{80}\text{Si}_{20}$ and $\text{Ni}_{81}\text{P}_{19}$ were prepared in the shape of ribbons (about 3 mm wide and 0.04 mm thick) by rapid quenching from the melt. The amorphous samples of $\text{Ni}_{81}\text{P}_{19}$ sheet (2 cm \times 3 cm \times 0.1 mm) were produced by electrodeposition onto a copper plate by applying the previously described method [9]. The sample composition was determined by chemical analysis.

The experimental apparatus, as well as the procedures for handling the X-ray scattering intensity, the correction of observed intensity data and their analysis, are essentially identical to the procedures employed in the previous works on the structure of metallic glasses [9] and high-temperature solids [10]. The low-temperature annealing and the creep test were carried out in vacuum of 10^{-5} Torr by applying a procedure similar to that of Kimura *et al.* [11].

We begin with a brief discussion of the uncertainty in the present structural data. The accumulated counts varying from 8×10^4 at low angles to 2×10^5 at high angles were chosen to hold the counting statistics approximately uniform. In addition, the normalization carried out to estimate the reduced interference function $i(Q)$ was in error by less than 0.8% on the basis of the usual Rahman method [12, 13]. Other sources of systematic error in X-ray diffraction of non-crystalline systems were identified by following the detailed discussion of Greenfield *et al.* [13]. Consequently, the total error in the reduced interference function obtained in this work is estimated to be 1.8%. We could suggest, however, that the relative changes, $Q\Delta i(Q)$, which are discussed in this work are in error by less than 0.5%, i.e. the accuracy of the relative changes is higher than that of the structure factor itself. The radial distribution function (RDF) $G(r)$ is calculated from the structure factor using the following equation:

$$G(r) = 4\pi r [\rho(r) - \rho_0] = \frac{2}{\pi} \int_0^\infty Q i(Q) \sin(Qr) dQ$$

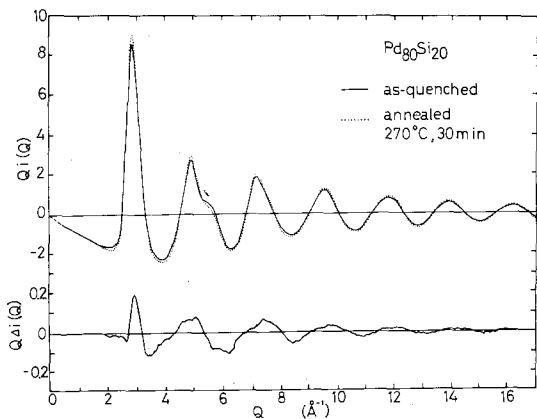


Figure 1 Interference function of sputtered $\text{Pd}_{80}\text{Si}_{20}$ amorphous alloy and the change in interference function caused by low-temperature annealing.

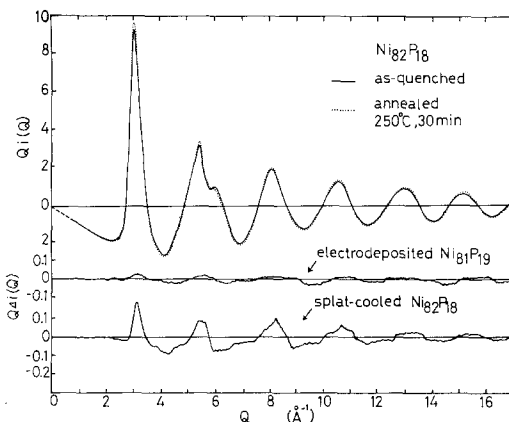


Figure 2 Interference function of sputtered $\text{Ni}_{82}\text{P}_{18}$ amorphous alloy and the change in interference function caused by low-temperature annealing together with that of electrodeposited $\text{Ni}_{81}\text{P}_{19}$ amorphous alloy.

where $\rho(r)$ is the radial density function and ρ_0 is the average number density. The uncertainties in the value of $G(r)$ and $\Delta G(r)$ are probably similar to those of $i(Q)$ and $\Delta i(Q)$, because it is confirmed that the computation errors in the Fourier transformation from $i(Q)$ to $G(r)$ have been reduced to a minimum by applying common procedures [14, 15].

3. Results and discussion

3.1. Effects of low-temperature annealing

The interference function $Q \cdot i(Q)$ and the change due to low-temperature annealing $Q \cdot \Delta i(Q)$ are shown in Figs. 1 and 2 for sputtered $\text{Pd}_{80}\text{Si}_{20}$ and $\text{Ni}_{82}\text{P}_{18}$, respectively. The annealing conditions are 270°C and 30 min for $\text{Pd}_{80}\text{Si}_{20}$, and 250°C and 30 min for $\text{Ni}_{82}\text{P}_{18}$. These annealing conditions

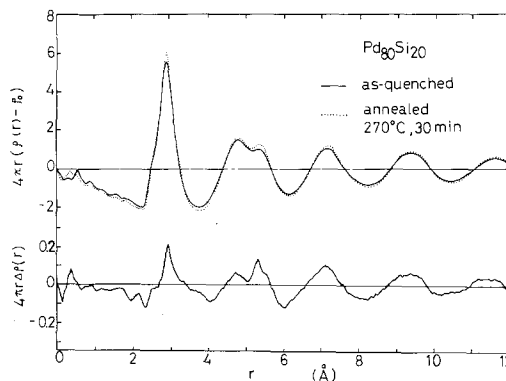


Figure 3 Radial distribution function of a sputtered $\text{Pd}_{80}\text{Si}_{20}$ amorphous alloy and the change in RDF caused by low-temperature annealing.

TABLE I Density, peak positions in the reduced interference function, $Qi(Q)$, and the radial distribution function, $G(r)$, and near neighbour numbers, n_1 , estimated from the area under the first peak of $G(r)$

		Density (g cm ⁻³)	$Qi(Q)$ (Å ⁻¹)			$G(r)$ (Å)			n_1 (atoms)
			1st	2nd	Shoulder	1st	2nd	Shoulder	
Pd ₈₀ Si ₂₀	As-quenched	10.62	2.82	4.85	5.62	2.81	4.69	5.29	11.4
	Annealed at 270° C for 30 min	10.66	2.82	4.83	5.60	2.81	4.68	5.33	11.6
	20% cold-rolled after annealed at 270° C for 30 min	10.63	2.81	4.83	5.61	2.82	4.67	5.28	11.2
	Annealed at 270° C for 30 min after 20% cold-rolled	10.67	2.82	4.83	5.62	2.81	4.68	5.32	11.5
	Direct cold-rolled of 35%	10.61	2.80	4.84	5.60	2.82	4.67	5.31	11.1
	Crept at 150° C for 600 min under 25 kg mm ⁻²	10.64	2.82	4.83	5.60	2.81	4.67	5.29	11.4
Ni ₈₁ P ₁₉	As-deposited	7.82	3.06	5.36	6.06	2.56	4.22	4.78	11.3
	Annealed at 250° C for 30 min	7.83	3.06	5.36	6.07	2.56	4.21	4.79	11.4
Ni ₈₂ P ₁₈	As-quenched	7.80	3.07	5.37	6.07	2.54	4.21	4.77	11.1
	Annealed at 250° C for 30 min	7.81	3.06	5.37	6.07	2.55	4.21	4.78	11.3

are known to induce substantial structural relaxation, but no crystallization [16, 17]. Fig. 2 also shows the change in $Q \cdot i(Q)$ of electrodeposited Ni₈₁P₁₉ caused by annealing at 250° C for 30 min. The radial distribution function $4\pi r [\rho(r) - \rho_0]$ and its change due to annealing, $4\pi r \Delta\rho(r)$, are shown in Figs. 3 and 4 for these alloys. The peak positions of $Qi(Q)$ and $G(r)$, and the density and co-ordination number are listed in Table I. The density was measured by the Archimedeian method with toluene.

The results shown here and the previous result on Fe₄₀Ni₄₀P₁₄B₆ [5] have a striking resemblance to each other, in spite of the differences in the alloy composition. The common features are as follows:

(1) the shape of $Qi(Q)$, and therefore $G(r)$, is common for all these alloys, with split second peak in both $Qi(Q)$ and $G(r)$, although there are quantitative differences primarily due to the different atomic sizes;

(2) the effect of annealing on $Qi(Q)$ and $G(r)$ is, in general, to increase the amplitude of the oscillation, rather than to change the positions of the peaks;

(3) the shoulder of the 2nd peak of $Qi(Q)$ is lowered by annealing;

(4) the relative changes in the heights of the first and second peaks in $G(r)$ are of the order of 2%, but the shoulder of the second peak and the third, fourth and fifth peaks are increased by more than 5% by annealing.

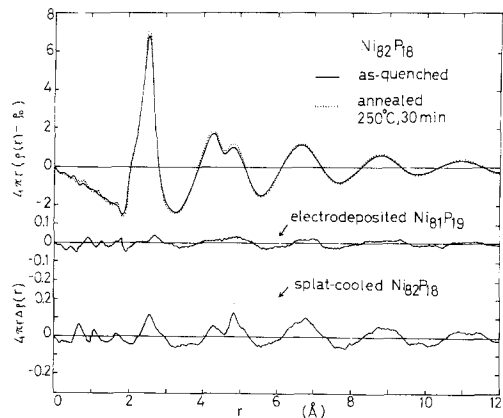


Figure 4 Radial distribution function of sputter-cooled Ni₈₂P₁₈ amorphous alloy and the change in RDF caused by low-temperature annealing together with that of electrodeposited Ni₈₁P₁₉ amorphous alloy.

Since the degree of relaxation depends upon the annealing conditions [5], it is not surprising that there are small variations among these three alloys in the magnitude of the change in $Qi(Q)$ or $G(r)$. However, the striking similarity in the salient features of the annealing effect clearly indicates that the conclusions obtained in the previous work [5] are probably valid for most of the transition metal-metalloid splat-cooled amorphous alloys. Namely, the structural relaxation is not just a densification [18], but involves a substantial short-range ordering via a highly collective atomic motion. The observed relaxation seems to be in a qualitative agreement with recent model calculations [19, 20], although there are differences in details.

For the electrodeposited $Ni_{81}P_{19}$, on the other hand, the effect of annealing is negligibly small and within the error of the measurement. This conclusion is in agreement with the previous study by Chi and Cargill [21], and indicates that the electrodeposited alloy is in a more relaxed state as produced, probably because the process is a very slow one.

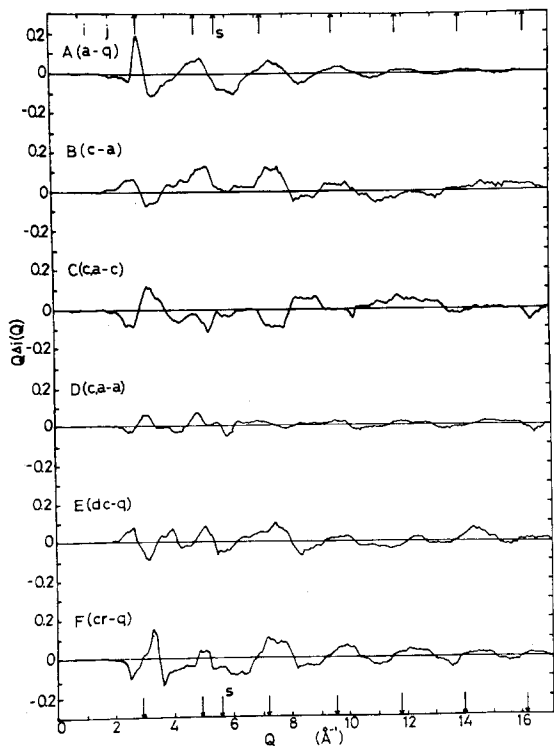


Figure 5 The change in interference function of splat-cooled $Pd_{80}Si_{20}$ amorphous alloy caused by low-temperature annealing, cold-rolling and isothermal creep.

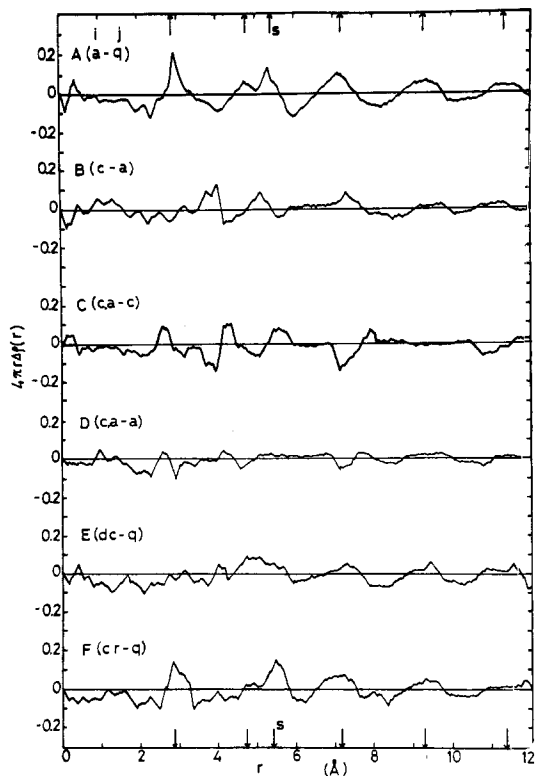


Figure 6 The change in radial distribution function of splat-cooled $Pd_{80}Si_{20}$ amorphous alloy caused by low-temperature annealing, cold-rolling and isothermal creep.

3.2. Effect of cold-rolling and isothermal creep

The experimental results for splat-cooled $Pd_{80}Si_{20}$ due to cold-rolling and isothermal creep are presented in Figs. 5 and 6 in terms of the relative changes in $Qi(Q)$ and $4\pi r\rho(r)$, respectively. For convenience, the profile of the relative change caused by low-temperature annealing is also shown in these figures. The notation for these figures is as follows: q, as-quenched; a, annealed at $270^\circ C$ for 30 min; c, 20% cold-rolled after annealing at $270^\circ C$ for 30 min; c, a, annealed at $270^\circ C$ for 30 min after 20% cold-rolling; dc, direct cold-rolling by 35% on the sample as-quenched; cr, crept at $150^\circ C$ for 600 min under 25 kg mm^{-2} . For example, the result labelled A(a-q) corresponds to the profile of structural relaxation due to low-temperature annealing. The arrows in these figures denote the positions of peaks in $Qi(Q)$ and $G(r)$. In addition, the arrow marked "s" indicates the position of the second peak shoulder.

The results of B(c, a-q) describe the effect of cold-rolling after annealing, while C(c, a-c)

corresponds to the changes induced by the further annealing afterwards. Except for five details, the relation $C(c, a - c) \simeq -B(c - a)$ appears to hold, so that $D(c, a - a)$ is almost negligibly small. This indicates that the deformation-induced changes in the structure can be recovered by subsequent annealing, in agreement with the observations made for other physical properties [6]. By comparing $B(c - a)$ and $-C(c, a - c)$, it should be possible to separate relevant features from the experimental noise. The most notable feature in $4\pi r \Delta\rho(r)$ is the peak at around 4 \AA , which has not been observed in the original RDF. This peak may be related to the one which appeared in the computer calculation by Boudreaux [22]. Furthermore, the split in the second peak becomes more smeared out. Thus the change induced by deformation appears to be quite distinct from the structural relaxation induced by annealing. It should be kept in mind that the deformation is usually highly localized around the shear bands, while the X-ray diffraction probes the entire volume. Therefore, the structural change within the shear band should be much greater than displayed here. At this moment, there is no structural model which can describe the change observed here.

The effect of cold-rolling on the as-quenched sample is given as $E(dc - q)$. There are some similarities between B and E; $E(dc - q)$ appears to have a slightly stronger oscillation in $4\pi r \Delta\rho(r)$ above 5 \AA , which might correspond to the conjecture that the deformation of as-quenched sample results both in the creation of shear band, and in the structural relaxation due to the pressure. However, it may be unwise to carry the discussion that far, since the experimental uncertainty may be larger than the difference between B and E. In any event, the effect of deformation is much smaller than has been previously reported [23].

The result shown as $F(cr - q)$ is much more similar to $A(a - q)$ than to $B(c - a)$, indicating that the structural change during isothermal creep is primarily due to the annealing, rather than the mechanical deformation. This suggests that the earlier stage of the mechanical creep (transient creep) is controlled by the structural relaxation. Further discussions of the creep behaviour from that point of view will be presented elsewhere.

Acknowledgements

The authors wish to acknowledge the important technical assistance of K. Yokoyama. This work was supported in part by the Army Research Office through Grant DAAG29-C-78-0017 to T.E. using the energy dispersive X-ray diffraction technique, and also by the National Research Council of Canada.

References

1. C. D. GRAHAM Jr and T. EGAMI, *Ann. Rev. Mat. Sci.* **8** (1978) 423.
2. S. E. PETRIE, in "Polymeric Materials" (American Society for Metals, Metals Park, 1975) p. 55.
3. Y. WASEDA and T. MASUMOTO, *Z. Phys.* **B22** (1975) 121.
4. T. EGAMI and T. ICHIKAWA, *Mat. Sci. Eng.* **32** (1978) 293.
5. T. EGAMI, *J. Mater. Sci.* **13** (1978) 2587.
6. R. S. WILLIAMS and T. EGAMI, *IEEE Trans. Mag. MAG-12* (1976) 927.
7. F. E. LUBORSKY, J. L. WALTER and D. G. LeGRAND, *ibid.* **MAG-12** (1976) 930.
8. Y. WASEDA and K. MORIYA, *Bull. Res. Inst. Min. and Met. Tohoku Univ. (Sendai)* **29** (1973) 135.
9. Y. WASEDA and S. TAMAKI, *Z. Phys.* **B23** (1976) 315.
10. Y. WASEDA, K. HIRATA and M. OHTANI, *High Temp. High Press.* **7** (1975) 221.
11. H. KIMURA and T. MASUMOTO, *Sci. Rep. RITU* **26A** (1977) 270.
12. A. RAHMAN, *J. Chem. Phys.* **42** (1965) 3540.
13. A. J. GREENFIELD, J. WELLENDFORD and N. WISER, *Phys. Rev.* **A4** (1971) 1607.
14. R. KAPLOW, S. L. STRONG and B. L. AVERBACH, *Phys. Rev.* **138** (1965) A1336.
15. A. H. NARTEN, D. M. DANFORD and H. A. LEVY, *J. Chem. Phys.* **46** (1967) 4875.
16. T. MASUMOTO and R. MADDIN, *Mat. Sci. Eng.* **19** (1975) 1.
17. Y. WASEDA, H. OKAZAKI and T. MASUMOTO, *J. Mater. Sci.* **12** (1977) 1927.
18. H. S. CHEN, *J. Appl. Phys.* **49** (1978) 3289.
19. L. V. HEIMENDAHL, *J. Phys. F* **5** (1975) L141.
20. R. YAMAMOTO, H. MATSUOKA and M. DOYAMA, *ibid.* **7** (1977) L243.
21. G. C. CHI and G. S. CARGILL III, *AIP Conf. Proc.* **31** (1976) 359.
22. D. S. BOUDREAUX, *Bull. Amer. Phys. Soc.* **23** (1978) 406.
23. T. MASUMOTO, H. KIMURA, A. INOUE and Y. WASEDA, *Mat. Sci. Eng.* **23** (1976) 141.

Received 31 August and accepted 6 October 1978.